Available online at www.sciencedirect.com

SCIENCE DIRECT

Vision Research 46 (2006) 1459–1472

Vision Research

www.elsevier.com/locate/visres

Partial preservation of rod and cone ERG function following subretinal injection of ARPE-19 cells in RCS rats

Y. Sauvé [a,b,*], I. Pinilla [b,c], R.D. Lund [b]

[a] *Departments of Ophthalmology and Physiology, 7-55 Medical Sciences Bldg, University of Alberta, Edmonton, Alta., Canada T6G 2H7*
[b] *Moran Eye Center, University of Utah, Salt Lake City, UT 84132, USA*
[c] *Servicio de Oftalmologia, Hospital Universitario Miguel Servet, P. Isabel La Catolica, 50004 Saragossa, Spain*

Received 8 April 2005; received in revised form 28 September 2005

Abstract

We quantified rod- and cone-related electroretinogram (ERG) responses following subretinal injections of the human-derived retinal pigment epithelial (hRPE) cell line ARPE-19 at age P23 to prevent progressive photoreceptor loss in the Royal College of Surgeons (RCS) rat. Culture medium-injected eyes served as sham controls. At P60, in comparison with sham-injected eyes, all recordings from hRPE-injected eyes showed preserved scotopic a- and b-waves, oscillatory potentials, double-flash-derived rod b-waves and photopic cone b-waves, and flicker critical fusion frequencies and amplitudes. Although the actual preservation did not exceed 10% of a-wave and 20% of b-wave amplitude values in non-dystrophic RCS and deteriorated rapidly by P90, rod- and cone-related ERG parameters were still recordable up to P120 unlike the virtually unresponsive sham-injected eyes.

Keywords: Retinal dystrophy; Preventive therapy; Photoreceptors; Functional evaluation; Scotopic threshold response

1. Introduction

Disorders affecting retinal pigment epithelial (RPE) cell function are associated with the secondary loss of photoreceptors. In humans, they are manifested as age-related macular degeneration (AMD) and some forms of retinitis pigmentosa (RP) caused by mutations in RPE-related genes, such as RPE65 (Gu et al., 1997; Marlhens et al., 1997; Maw et al., 1997; Petrukhin et al., 1998) and Mertk (Gal et al., 2000; McHenry et al., 2004; Thompson et al., 2002). One of the approaches being developed as a potential treatment for these disorders is to replace the defective RPE with normal cells, either freshly harvested or maintained as cell lines. The most extensively used animal model for such studies is the RCS rat, which has a recessive mutation in the Mertk receptor tyrosine kinase gene (D'Cruz et al., 2000; Nandrot et al., 2000) that largely precludes RPE cells from phagocytosing shed rod outer segments and this results in the formation of a debris zone, destruction of outer segments, and finally death of photoreceptors (Bourne, Campbell, & Tansley, 1938; Dowling & Sidman, 1962). This gene defect is orthologous to a form of RP (Gal et al., 2000), and by virtue of the primary defect being in the RPE cells, it may serve as an analogous model of some aspects of AMD. A series of studies has shown that subretinal injections of cells from human RPE (hRPE) cell lines not only rescue photoreceptors anatomically but also preserve visual function in RCS rats (Girman, Wang, & Lund, 2003, 2005; Lund et al., 2001; McGill et al., 2004; Sauvé, Girman, Wang, Keegan, & Lund, 2002; Sauvé, Lu, & Lund, 2004). However, it remains unclear how anatomical preservation translates into respective function of rod and cone pathways. This can be assessed using ERG.

Full field corneal ERG is routinely used clinically to measure and dissect rod- from cone-driven retinal activity (Fishman, Birch, Holder, & Brigell, 2001). Its application in

* Corresponding author. Tel.: +780 492 8609.
E-mail address: ysauve@ualberta.ca (Y. Sauvé).

0042-6989/$ - see front matter © 2005 Elsevier Ltd. All rights reserved.
doi:10.1016/j.visres.2005.11.009

rodents is well established (for reviews see: Nusinowitz, Ridder, & Heckenlively, 2002; Peachey & Ball, 2003) and has proven useful for monitoring the progression of retinal degeneration (Pinilla, Lund, & Sauvé, 2004) and assessing the potential benefit of experimental interventions such as cell-based therapies (Pinilla, Lund, Lu, & Sauvé, 2005; Pinilla, Lund, & Sauvé, 2005; Sauvé et al., 2004). In this study, we used a series of full field ERG protocols to evaluate the functional state of rod and cone pathways. Our findings indicate that subretinal injections of cells from an hRPE line can partially preserve both rod and cone ERG function. However, ERG responsiveness is abnormal for both rod- and cone-driven parameters, and shows signs of decline with post-operative time, especially from P60 to P90. Dysfunctional phototransduction as well as circuitry remodeling in the retina are likely involved in the pathological ERG responsiveness and its progressive decline over time.

2. Experimental procedures

2.1. Animals

This work was done in dystrophic (RCS rdy^+ p^+, $n = 24$) and non-dystrophic congenic (RCS rdy^- p^+, $n = 4$) pigmented RCS rats, which were bred in a colony at the University of Utah, and maintained under a 12-h light/dark cycle (light cycle mean illumination: 30 cd/m^2). All animals were housed and handled with the authorization and supervision of the Institutional Animal Care and Use Committee from the University of Utah. Every procedure conformed to the National Institute of Health Guide for the Care and Use of Laboratory Animals (NIH Publications No. 80-23) revised 1996. The procedures also conformed to the ARVO Statement for the Use of Animals in Ophthalmic and Vision Research. All efforts were made to minimize the number of animals used and any potential discomfort.

2.2. Subretinal transplantation

At age P21–23, dystrophic RCS rats received subretinal injections of a suspension of human RPE cells (spontaneously arising ARPE-19 line from American Type Culture Collection, ATCC, reference number: CRL-2302) as previously described (Lund et al., 2001; Sauvé et al., 2002). In brief, following anesthesia with xylazine–ketamine (1 ml/kg i.p. of the following mixture: 2.5 ml xylazine at 20 mg/ml, 5 ml ketamine at 100 mg/ml, and 0.5 ml distilled water), dystrophic RCS rats received injections of cells ($n = 12$) or medium alone ($n = 12$). Cultures of ARPE-19 cells were trypsinized, washed, and delivered as a suspension (2×10^5 cells per injection) in 2 μl of Ham's F10 medium through a fine glass pipette (internal diameter 75–150 μm) into the eye via a tiny scleral incision. All injections were made in the upper temporal retina of the right eye: the left eye served as the untreated control. All animals received daily dexamethasone injections (1.6 mg/kg, i.p.) for 2 weeks and were maintained on cyclosporine administered in the drinking water (210 mg/L; resulting blood concentration: 250–300 μg/L; Coffey et al., 2002) from 2 to 3 days prior transplantation until sacrifice. A separate study (Raibon, Roger, & Lund, 2003; E. Raibon, unpublished results) has shown that this treatment regimen reduces the microglial activation, normally evident in un-operated RCS rats.

2.3. ERG recordings

Animals were prepared under dim red light following overnight dark adaptation, and ERGs obtained as previously described (Pinilla et al., 2004). At P60, ERGs were recorded for two congenics, the 12 hRPE-injected animals, and the 12 sham-injected animals; after which four of the hRPE-injected animals and six of the shams were culled and used for anatomy (Lund et al., 2004). At P90, two additional congenics, and the remaining eight hRPE-injected animals and six shams were recorded again for ERGs; two of the cell-injected and two of the sham animals were culled for anatomical analysis. Finally, the six remaining hRPE-injected and four sham animals were recorded for ERG at P120 and then all were culled for anatomical analysis (Lund et al., 2004).

2.3.1. Mixed scotopic ERG responses

Recordings consisted of three to five single flash presentations (standard duration of 10 μs). Stimuli were presented at 16 increasing intensities varying from −3.7 to 2.86 log cds/m^2 in luminance. To minimize the occurrence of incomplete photopigment regeneration and incomplete recovery from flashes mediated by the downstream transduction biochemistry (which could reduce the b-wave amplitude on successive flashes), interstimuli intervals (ISI) were increased as the stimulus luminance was elevated from 10 s at the lowest stimulus intensity up to 2 min at the highest stimulus intensity. Choice of the intervals was defined in pilot experiments (Pinilla et al., 2004). The observation by Perlman (1978) of slower photopigment regeneration also prompted us to do other pilot experiments in order to control for the potential bleaching effects throughout the course of the testing session. In the same animal, scotopic b-wave amplitude was measured at the beginning of a recording session using a 1.4 log cds/m^2 intensity flash, followed by standard intensity response series. The amplitudes to this same intensity obtained prior to and during the intensity series were not statistically different when considering six animals at P60 and P90, suggesting that slower pigment regeneration does not contribute to changes over the time span of the recording session.

The maximal b-wave amplitude was that obtained during the flash intensity series, regardless of the specific stimulus intensity. Criterion amplitudes were established at 10 μV for a-waves and b-waves. The amplitude of the b-wave was measured from the a-wave negative peak up to the b-wave positive apex, and not up to the peak of oscillations, which can exceed the b-wave apex (Nusinowitz et al., 2002).

OPs were extracted offline from records obtained with standard filtering (0.3–500 Hz). We relied on the EM for Windows software from LKC, which relies on fast Fourier transform to extract events occurring at frequencies of 75 Hz and higher.

2.3.2. Isolation of dark-adapted rod and cone responses using a double-flash protocol

A double-flash protocol, similar to that described previously in RCS rats (Pinilla et al., 2004) and other rodents (Birch, Hood, Nusinowitz, & Pepperberg, 1995; Lyubarsky, Falsini, Pennesi, Valentini, & Pugh, 1999; Nixon, Bui, Armitage, & Vingrys, 2001), was used to isolate rod and cone ERG components. In brief, a probe flash was presented 1 s after a conditioning flash (1.4 log cds/m^2). The role of the conditioning flash in this paradigm was to transiently saturate rods so that they were rendered unresponsive to the probe flash. Response to the probe flash was taken as reflecting cone-driven activity. A rod-driven b-wave was derived by subtracting the cone-driven response from the mixed response (obtained following presentation of a probe flash alone, without a precedent conditioning flash). By varying the intensity of the probe flash, it was possible to obtain isolated cone intensity responses.

Averages of up to three traces were obtained for each stimulus condition: intervals between double-flash presentations were set at 2 min to allow near-complete recovery of rod responsiveness.

2.3.3. Photopic ERG responses

After testing under scotopic adaptation conditions, rats were light adapted for 20 min with a background illumination of 30 cd/m^2 to reach a stable photopic-response level (Gouras & MacKay, 1989; Peachey, Goto, al-Ubaidi, & Naash, 1993). To confirm the stability of responses after 20 min light adaptation we did pilot experiments in P60 non-dystrophic and dystrophic RCS rats where the 20 Hz flicker amplitude was measured at 5-min intervals following transition from scotopic to photopic (30 cd/m^2) adaptation. Amplitude values increased

from time 0 to 15 min and remained stable onward. Furthermore, to confirm the stability of responsiveness during the photopic testing session, we did similar pilot experiments as described under scotopic conditions, that is, photopic b-wave amplitude was measured to a 1.4 log cds/m^2 intensity flash, prior and during standard photopic intensity-response series. No statistical differences were seen between the two measures when considering six animals at P60 and P90, confirming the observation made under scotopic conditions suggesting that slower pigment regeneration does not contribute to changes over the time span of the recording session.

Photopic intensity responses (30 cd/m^2 background) ranged from −1.6 to 2.9 log cds/m^2 (−1.6, −0.6, 0.4, 1.4, 2.4, and 2.9 log cds/m^2). Flicker responses were recorded to white strobe flash presentations in a ganzfeld stimulator with a luminance of 31.5 cds/m^2. Flash intensity was set to 1.4 log cds/m^2. Stimuli were presented at 3 Hz, and then at 5 Hz up to 50 Hz in 5-Hz steps. The critical fusion frequency (CFF) was set as the value of X when Y equals 3 μV on plots of log flicker amplitude versus flicker frequency. When the CFF was achieved, lower frequencies were studied; 40 responses were averaged.

2.3.4. Recovery from conditioning flash

Finally, we examined the recovery phase of the b-wave following bleaching with a conditioning flash (1.4 log cds/m^2). This was achieved by recording the responses to a test flash (1.4 log cds/m^2) presented at increasing intervals following the presentation of the conditioning flash. Experiments were done under scotopic adaptation (as the last scotopic tests) and repeated following photopic adaptation conditions (after photopic intensity-response, prior to flicker testing). The delays studied consisted of: 30, 60, 120, 240, 480, 960, 2000, 4000, and 8000 ms.

2.3.5. Statistics

Errors are expressed as standard errors of the mean (SEM). Comparisons between two different groups were made using: (1) Student's t test when data followed normal distributions; and (2) Mann–Whitney U test when data did not follow a normal distribution. The probability level at which the Null Hypothesis was rejected was set at $p < 0.05$.

3. Results

3.1. Non-dystrophic RCS rats

Four congenic animals provided background data for the experimental studies: two animals were tested at P60 and two at P90, but since the response properties were similar at the two time points, results were pooled. Fig. 1 summarizes the results. Thresholds for scotopic a-waves were at −2.44 log cds/m^2. The amplitude of the a-wave increased with stimulus intensity reaching maximal values (628 ± 66 μV) to the penultimate intensity tested (2.39 log cds/m^2), with no significant diminution in amplitude between this and the highest intensity tested (2.86 log cds/m^2) (Fig. 1A). The b-wave amplitude was already 247 ± 33 μV at the lowest intensity tested (−3.70 log cds/m^2) and a peak amplitude of 1371 ± 33 μV was recorded at 1.89 log cds/m^2 without further significant decrements up to the highest intensity tested (Fig. 1B). There were two distinct rising phases in the intensity responses for mixed scotopic b-waves (Fig. 1B) as well as for double-flash-isolated rod b-waves (Fig. 1C). The latter showed similar amplitude responses for −3.70 to −1.63 log cds/m^2 as mixed b-waves, indicating pure rod responses at these low levels. With increased luminance (starting from −1.22 log cds/m^2 and higher), rod b-waves increased more slowly in amplitude than mixed b-waves, peaking 1034 ± 56 μV at 1.89 log cds/m^2. Isolated dark-adapted cone b-wave amplitudes (Fig. 1D) reached a plateau at 0.38 log cds/m^2: this compared with photopic b-wave intensity responses (Fig. 1E). However, thresholds were lower and maximal amplitudes were larger for isolated dark-adapted cone responses in comparison with photopic b-waves. With regard to flicker ERG (Fig. 1F), an approximately linear relationship was observed when plotting the log response amplitude against the flicker frequency. The function that best fitted this relationship was of the exponential type: $y = ce^{bx}$; giving a coefficient of correlation R^2 of 0.9904. Flicker amplitudes were maximal (362 ± 119 μV) at 3 Hz, the lowest frequency tested and fused at 42.4 Hz. In experiments involving the dynamic of recovery from a conditioning flash, initial recovery of mixed b-waves (Fig. 1G) began at 120 ms and full recovery (amplitudes reaching normalized values of one) was still incomplete at 10 s. Under photopic conditions (Fig. 1H), b-wave recovery from the conditioning flash began at 60 ms and full recovery was achieved in a further 60 ms.

3.2. Dystrophic RCS rats: Sham-injected eyes

As in previous studies in untreated dystrophic eyes (Bush, Hawks, & Sieving, 1995; Pinilla et al., 2004; Sauvé et al., 2004), already by P60, a-waves could no longer be elicited and b-wave amplitudes just barely reached criterion levels in sham-injected eyes. No b-waves could be elicited by P90; the only ERG responses recorded at P90 or P120 were elicited by flicker stimuli. Therefore, detailed analysis of most ERG parameters in sham-injected eyes was limited to P60. Data from sham-injected eyes are presented below in order to make direct comparisons with data from cell-injected eyes for the respective ERG parameters studied here.

3.3. Dystrophic RCS rats: Cell-injected eyes

3.3.1. Mixed scotopic responses

It is clear from the scotopic intensity responses obtained at P60 that hRPE injections lead to the preservation of both mixed a- and b-waves when compared with sham injections (Fig. 2A). While no a-waves could be recorded in sham-injected eyes at P60, a-waves could be elicited up to P120 in all hRPE-injected eyes (Figs. 2A and B). At P60, a-wave threshold was −1.63 log cds/m^2; a-wave amplitude increased with stimulus intensity, reaching maximal values (33 ± 6 μV) at 1.37 log cds/m^2, and slightly decreasing thereafter. By P90 and P120, a-wave thresholds were increased to −1.22 and −0.81 log cds/m^2, respectively, and the maximum amplitude was stable at 11 ± 5 and 8 ± 6 μV over a wide range of stimulus intensities never exceeding the value of about 20 μV reported for the cone a-wave in intact rodents (Lyubarsky et al., 1999; Xu, Ball, Alexander, & Peachey, 2003).

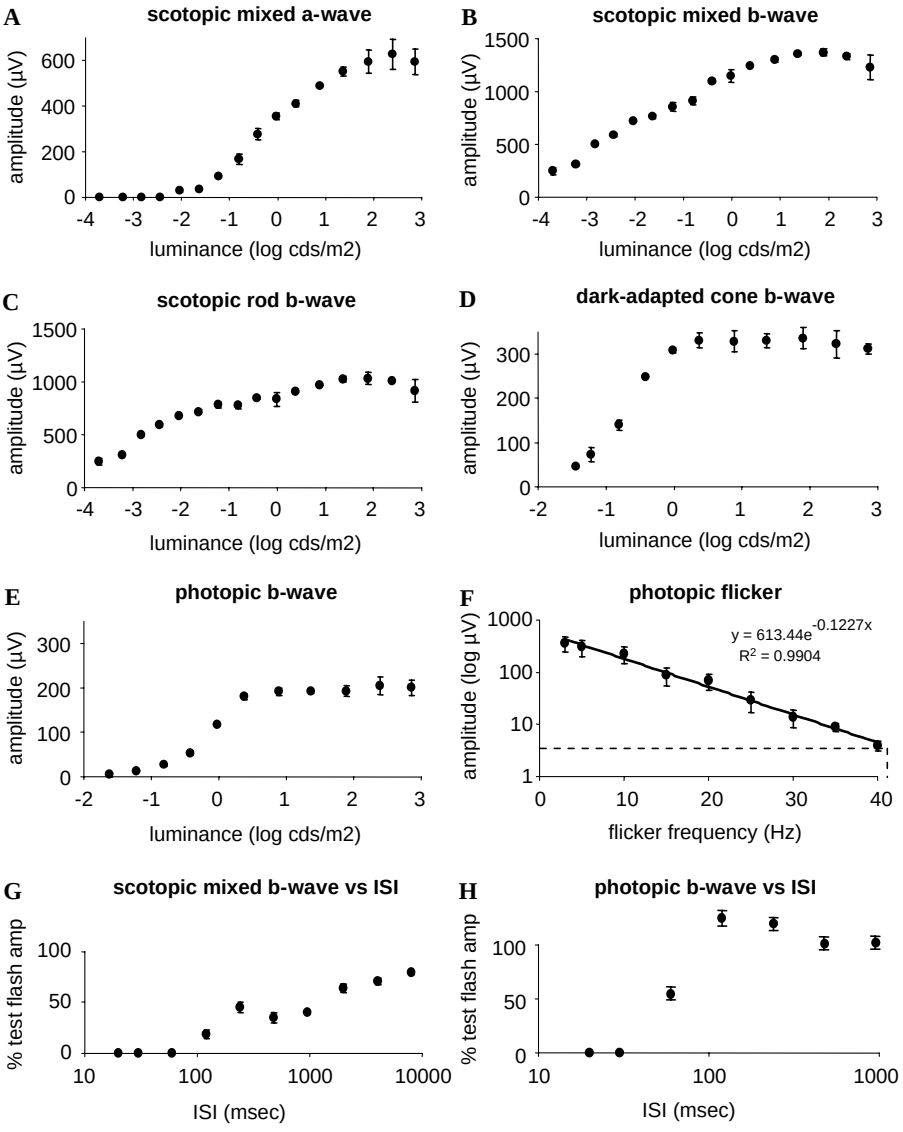

Fig. 1. Summary of the results obtained in four non-dystrophic RCS rats ($n = 2$ at P60; $n = 2$ at P90; data pooled), using all the various ERG tests that were applied in the present study. The first five panels show ERG amplitude versus flash intensity (V–log I) series of mixed scotopic a-waves (A), mixed scotopic b-waves (B), double-flash-isolated scotopic rod b-waves (C), double-flash-isolated dark-adapted cone responses (D), and photopic responses (E). (F) The amplitude (on a log scale) of the flicker ERG response as a function of stimulus frequency; the dotted line points to the 3 μV amplitude criterion for CFF and corresponding frequency value. Finally, the two last panels show the time course of b-wave recovery from a conditioning flash under scotopic (G) and photopic (H) adaptation. Error bars represent the standard error of the mean.

The center column of Fig. 2A shows average intensity-response curves for mixed b-wave responses (see Fig. 2B for examples of individual traces). At P60, amplitudes increased with stimulus intensity reaching a plateau (with maximal intensity at $-0.02\,\log\,cds/m^2$) and then decreasing progressively, with values getting significantly lower at the two highest intensities tested (2.39 and $2.86\,\log\,cds/m^2$). b-Wave amplitudes were higher than in sham-injected eyes throughout the whole range of intensities tested with the exception of the lowest level ($-3.7\,\log\,cds/m^2$); however, at this level, b-wave response amplitudes surpassed the criterion level of 10 μV only in hRPE-injected eyes. The highest amplitude ($136 \pm 36\,\mu V$) far exceeded the best response in sham-injected eyes ($15 \pm 9\,\mu V$) although it represented only 10% of the maximal mixed b-wave amplitude in non-dystrophics. In comparison with P60, there was a severe drop in maximal mixed b-wave amplitudes at P90 and these were reached at lower luminance intensities ($37 \pm 10\,\mu V$ at $-1.22\,\log\,cds/m^2$). The plateau defined by mixed b-wave amplitude values that did not differ statistically from the maximal value became wider. Similar wide plateaus were seen in sham-injected eyes at P60, where there was no clear intensity-response relationship: mixed b-wave amplitudes just barely exceeded the 10 μV criterion level and the values obtained from most of the range tested did not vary statistically significantly ($11.5 \pm 5\,\mu V$ at $-2.04\,\log\,cds/m^2$ to $12.5 \pm 8.5\,\mu V$ at $1.89\,\log\,cds/m^2$). By P120, mixed b-waves could still be recorded in cell-injected eyes, giving

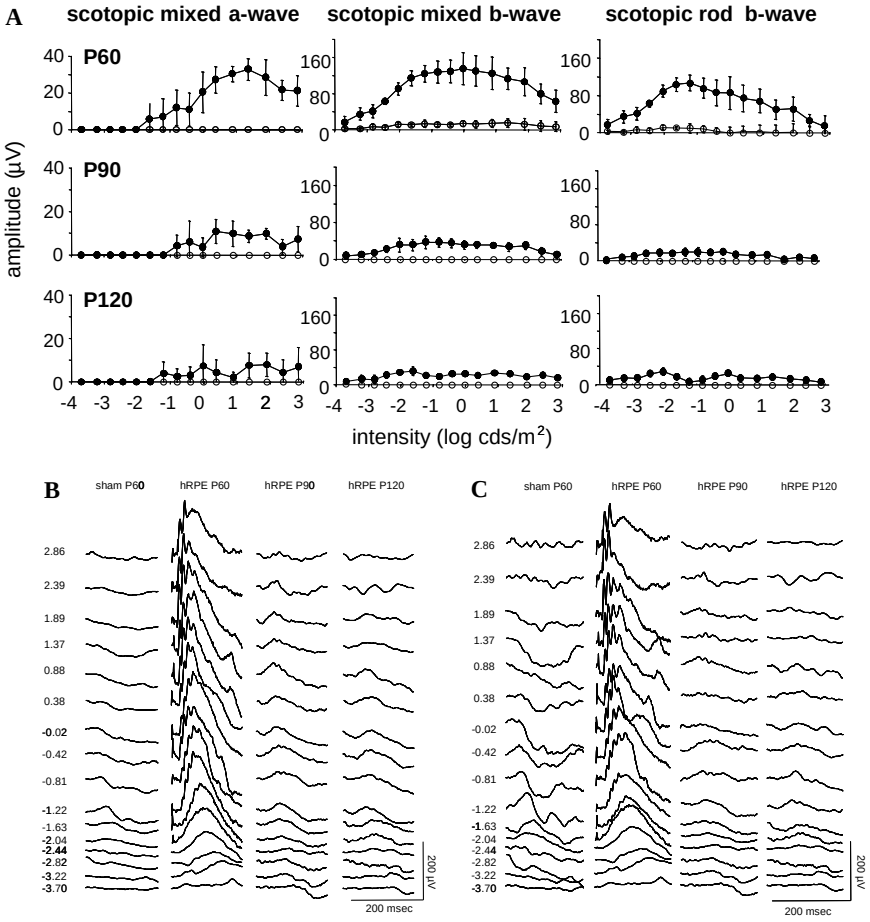

Fig. 2. (A) ERG amplitude versus flash intensity (V–log I) series of mixed scotopic a-waves (left column), mixed scotopic b-waves (center column), and double-flash-isolated scotopic rod b-waves (right column) for animals recorded longitudinally at ages P60, P90, and P120 (presented along respective rows). Filled circles: hRPE-injected eyes; unfilled circles: sham-injected eyes. Note the drop in maximal amplitude (for all components) between P60 and P90 in hRPE-injected eyes. (B) Examples of mixed scotopic ERG responses recorded from a sham-injected eye recorded at P60 and from a hRPE-injected eye at P60, P90, and P120. Traces from respective intensity series are displayed in columns, from dimmest (bottom) to brightest (top). Stimulus flash intensities (in log cd/m^2) are indicated along the left side. Preservation of higher amplitude responses can be seen when comparing the hRPE-injected eye (recorded at any age) with the sham-injected eye (recorded at P60). However, severe drop in amplitude can be seen between P60 and P90 in the hRPE-injected eye. (C) Examples of double-flash-isolated rod scotopic ERG responses recorded from the same animals and at the same time points as presented in Fig. 2. Traces from respective intensity series are displayed in columns, from dimmest (bottom) to brightest (top). Stimulus flash intensities (in log cd/m^2) are indicated along the left side. Preservation of higher amplitude responses can be seen when comparing the hRPE-injected eye (recorded at any age) with sham-injected eye (recorded at P60), despite the severe drop in amplitude between P60 and P90 in the hRPE-injected eye. Note the negative component (STR-like) seen in the sham-injected eye at P60 but not noticeable in the hRPE-injected even at P120. Error bars represent the standard error of the mean.

intensity-response curves that were similar to those obtained at P90. Maximal b-wave amplitudes were also reached at lower luminance than at P60 ($31 \pm 10\,\mu V$ at $-1.63\,\log cds/m^2$).

Oscillatory potentials were elicited only in hRPE-injected eyes (Fig. 3). The average amplitude to a flash of $1.37\,\log cds/m^2$ was $158 \pm 32\,\mu V$ in hRPE-injected eyes, in comparison with $622 \pm 47\,\mu V$ in age-matched non-dystrophic RCS rats. The proportion of OP amplitude rescued was further decreased with age, from 25% at P60 to 8% at P90 and 7% at P120. No differences in timing were seen between hRPE-injected eyes and non-dystrophics at P60 with regard to the onset of the first oscillation (28–30 ms) and last oscillation (77–82 ms); however, there were clear delays in onset of the first oscillation at P90 and P120 in hRPE-injected eyes (39–43 ms). The timing of last oscillations became extremely variable due to lower occurrence of oscillations following the first one.

3.3.2. Double-flash protocol

3.3.2.1. Isolated rod scotopic responses. Using a double-flash technique, we dissected both rod and cone contributions to the mixed scotopic b-wave. The results indicated that hRPE injections preserved rod-driven responses when compared with sham injections. Fig. 2A (right column) shows average intensity-response curves for double-flash-isolated rod b-waves (see Fig. 2C for examples of individual isolated rod responses). At P60, rod-driven responses were significantly higher in hRPE-injected eyes (maximum of $108 \pm 17\,\mu V$) than in shams (maximum of $11 \pm 3\,\mu V$) and

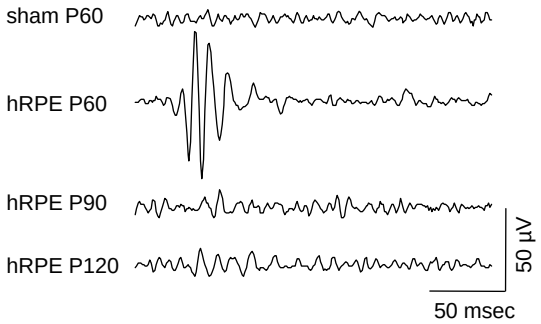

Fig. 3. Examples of oscillatory potentials elicited by a 1.37 log cds/m^2 flash under scotopic conditions. Traces correspond to the mixed scotopic responses presented in Fig. 2 (see traces at 1.37 log cds/m^2). Note the absence of oscillatory potentials in the sham-injected eye at P60. Injection of hRPE cells resulted in preserved oscillatory potentials at P60 but not after.

persisted up to the oldest age tested (P120), with an average maximal value of $22 \pm 6\,\mu V$ that still exceeded at P120 the average maximal value recorded in shams at P60. When compared with mixed scotopic b-waves, isolated rod b-waves reached maximal amplitudes at lower stimulus intensities and were severely reduced in amplitude as the stimulus intensity was increased ($13 \pm 24\,\mu V$ at 2.86 log cds/m^2 compared with $108 \pm 17\,\mu V$ maximal value reached at -1.22 log cds/m^2) despite using 2 min ISI. Because we were concerned whether 2 min was sufficiently long between tests, we extended the ISI up to 10 min in two animals with little change in amplitude (not illustrated). The intensity at which maximal rod b-wave amplitudes were reached shifted to lower levels with age in hRPE-injected animals (-1.63 log cds/m^2 at P120 compared with -0.02 log cds/m^2 at P60).

In all sham-injected animals, as the stimulus intensity increased, b-waves were progressively replaced by negative going components (see Fig. 2C, right column), analogous to the high threshold scotopic threshold responses (STRs) previously reported in RCS rats (Bush et al., 1995). As was the case for rod-driven components, this STR-like component was transiently bleached under the double-flash conditions used here. Such STR-like responses were seen in only one hRPE-injected animals recorded at P120 (Fig. 2C). In this single instance, the amplitude of these negative deflections was considerably less than in shams at P60 and their duration much shorter.

3.3.2.2. Isolated dark-adapted cone responses. Cone-driven responses were also preserved in cell-injected eyes, compared with sham injections. Fig. 4 (left column) shows averaged intensity-response curves for double-flash-isolated dark-adapted cone b-waves (see Fig. 4B for examples of individual dark-adapted cone responses). At P60, b-wave thresholds were lower for hRPE-injected eyes (-1.63 log cds/m^2) compared with shams (-0.42 log cds/m^2) and amplitudes were significantly higher in hRPE-injected eyes (maximum of $63 \pm 16\,\mu V$) compared with shams (maximum of $20 \pm 5\,\mu V$), but represented only 20% of the maximal isolated dark-adapted cone b-wave amplitude in non-dystrophics. Amplitudes increased with stimulus intensity, peaking at 1.37 log cds/m^2 in hRPE-injected eyes but at a much lower level (-0.02 log cds/m^2) in shams. While shams were only responsive at P60, hRPE-injected eyes retained dark-adapted cone b-waves up to the oldest age tested, P120. However, from P60 to P90, there was a significant decrease in maximal amplitudes in hRPE-injected eyes (down to $23 \pm 3\,\mu V$) and plateaus were reached at lower intensities, as was the case in shams at P60. Dark-adapted cone b-waves remained stable in amplitude from P90 up to P120, with an average maximal value of $25 \pm 6\,\mu V$.

3.3.3. Single flash photopic responses

Photopic intensity responses (presented in Fig. 4A, right column) gave results comparable to double-flash-isolated dark-adapted cone responses. Averaged intensity-response curves for photopic b-waves (see Fig. 4C for examples) are presented in Fig. 4A (right column). At P60, b-wave thresholds were lower for hRPE-injected eyes (-1.63 log cds/m^2) compared with shams (-0.81 log cds/m^2). Amplitudes increased with stimulus intensity, peaking at 1.37 log cds/m^2 in hRPE-injected eyes but at a much lower level (-0.42 log cds/m^2) in shams. Maximum b-wave amplitudes were significantly higher in hRPE-injected eyes ($43 \pm 9\,\mu V$) compared with shams ($15 \pm 8\,\mu V$). Photopic b-waves could only be elicited at P60 in sham-injected eyes, but persisted in hRPE-injected eyes up to P120, with an average maximal value of $16 \pm 2\,\mu V$ at P90 and of $13 \pm 3\,\mu V$ at P120. As with most parameters analyzed, maximal photopic b-wave amplitudes were significantly decreased from P60 to P90 in hRPE-injected eyes and plateaus were reached at lower intensities, as was the case in shams at P60.

3.3.4. Photopic flicker responses

We have applied the photopic flicker ERG approach to further characterize cone function. Both hRPE- and sham-injected RCS rats gave stable and repeatable recordings. There was no evidence of response fatigue over time: tests done before and after presentation of flicker stimuli covering the full range of frequencies gave essentially similar results. Examples of averaged records for various stimulus frequencies are shown in Fig. 5A. In all animals, at all ages, response amplitudes were maximal at 3 Hz and progressively decreased with presentation of higher frequency stimuli. At low frequency stimulation (3 and 5 Hz), the waveform typically showed a positive deflection reaching maximal amplitude of 60 ms after the stimulus artifact, followed by a smaller amplitude negative deflection. At P60, oscillatory potentials could be seen at the crest of each positive deflection in both hRPE (at 3 and 5 Hz)- and sham (at 3 Hz only)-injected eyes. By P90, oscillatory potentials were no longer seen in shams, but persisted in hRPE-injected eyes at 3 Hz in all animals and at 5 Hz in three of the eight animals tested at that age. By P120, oscillatory potentials could no longer be elicited in hRPE-injected eyes.

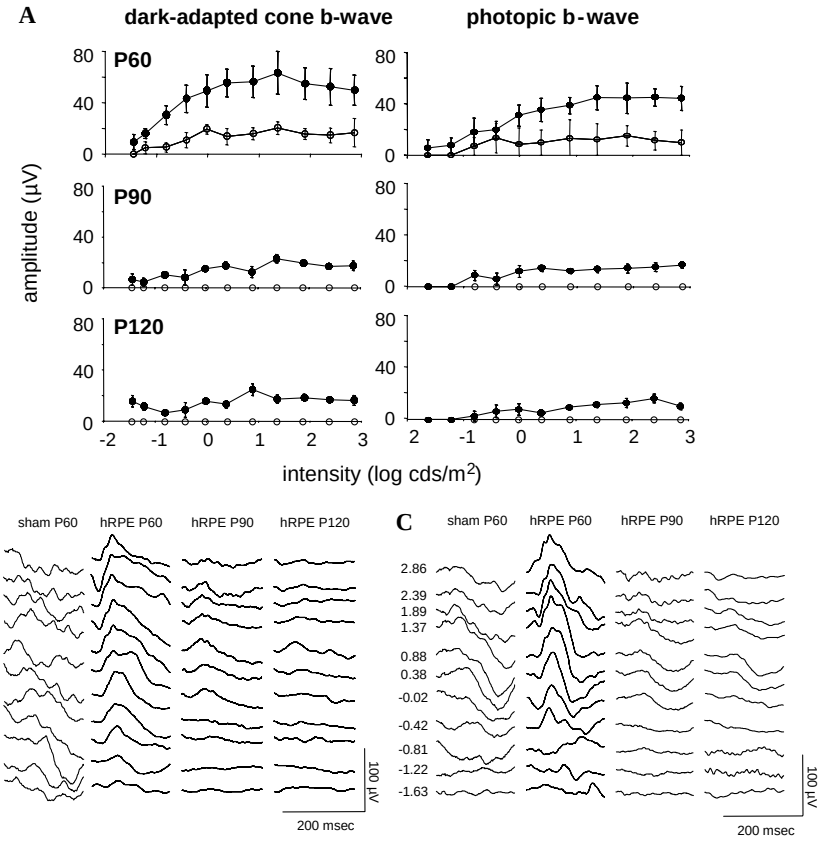

Fig. 4. (A) ERG b-wave amplitude versus flash intensity (V–log I) series of double-flash-isolated dark-adapted cone responses (left column) and photopic responses (right column) for animals recorded longitudinally at ages P60, P90, and P120 (presented along respective rows). Black circles: hRPE-injected eyes; white circles: sham eyes. Statistically significant higher amplitudes were seen at all ages for all ERG components when comparing results from hRPE-injected with those from age-matched sham-injected eyes. (B) Examples of double-flash-isolated dark-adapted cone responses recorded from the same animals and at the same time points as presented in Fig. 2. Traces from respective intensity series are displayed in columns, from dimmest (bottom) to brightest (top). Stimulus flash intensities (in log cds/m^2) are indicated along the left side. Preservation of highest amplitude responses can be seen at all time points when comparing hRPE-injected eyes with age-matched sham-injected eyes. Note the drop in b-wave amplitude between P60 and P90. (C) Examples of photopic responses recorded from the same animals and at the same time points as presented in Fig. 2. Traces from respective intensity series are displayed in columns, from dimmest (bottom) to brightest (top). Stimulus flash intensities (log cds/m^2) are indicated along the left side. Preservation of higher amplitude responses can be seen when comparing the sham-injected eye at the P60 time point with age-matched hRPE-injected eye. Note that the amplitude of the b-wave drops considerably between P60 and P90 in the hRPE-injected eye. Error bars represent the standard error of the mean.

Fig. 5B shows the log response amplitude against the flicker frequency. At P60, for hRPE-injected eyes, values of maximal flicker amplitude ($94 \pm 11\,\mu V$) and 20 Hz amplitude ($12 \pm 5\,\mu V$) were both significantly higher than for sham-injected eyes (49 ± 4 and $0.5 \pm 0.7\,\mu V$, respectively). The coefficient of correlation values (R^2) were higher in hRPE-injected (0.98) compared with sham-injected (0.95) animals. The constant "c" (corresponding to the extrapolated amplitude value at the ordinate origin) also tended to be higher in hRPE-injected animals (188 ± 22) than in sham-injected animals (162 ± 17), but this difference was not statistically significant. The slope of these curves (related to the variable "b") was statistically significantly steeper in shams (-0.27 ± 0.04) compared with hRPE-injected animals (-0.15 ± 0.02), and CFF were significantly higher in hRPE-injected animals (27 ± 4 Hz) than in sham-injected animals (14 ± 2 Hz). At P90, while all flicker parameter values dropped significantly for both groups, respective values remained significantly higher for hRPE-when compared with sham-injected eyes; for example, $39 \pm 5\,\mu V$ versus $26 \pm 7\,\mu V$ for maximal flicker amplitude and 21 ± 2 Hz versus 13 ± 4 Hz for CFFs. By P120, there was a further drop in all flicker parameter values, but significantly higher values were still seen in hRPE-injected eyes when compared with sham-injected eyes: $21 \pm 4\,\mu V$ versus $10 \pm 3\,\mu V$ for maximal flicker amplitude and 20 ± 3 Hz versus 11 ± 3 Hz for CFFs.

3.3.5. Dynamic of b-wave recovery from conditioning flash

When tested at P60, unveiling of a b-wave occurred at shorter intervals in sham-injected eyes compared with hRPE-injected eyes. This was the case under both scotopic and photopic adaptation (Fig. 6). At short intervals between the two flashes, the apparent downward shift in baseline was due to the presence of the b-wave elicited from the first flash; the slope of this shift was proportional to the

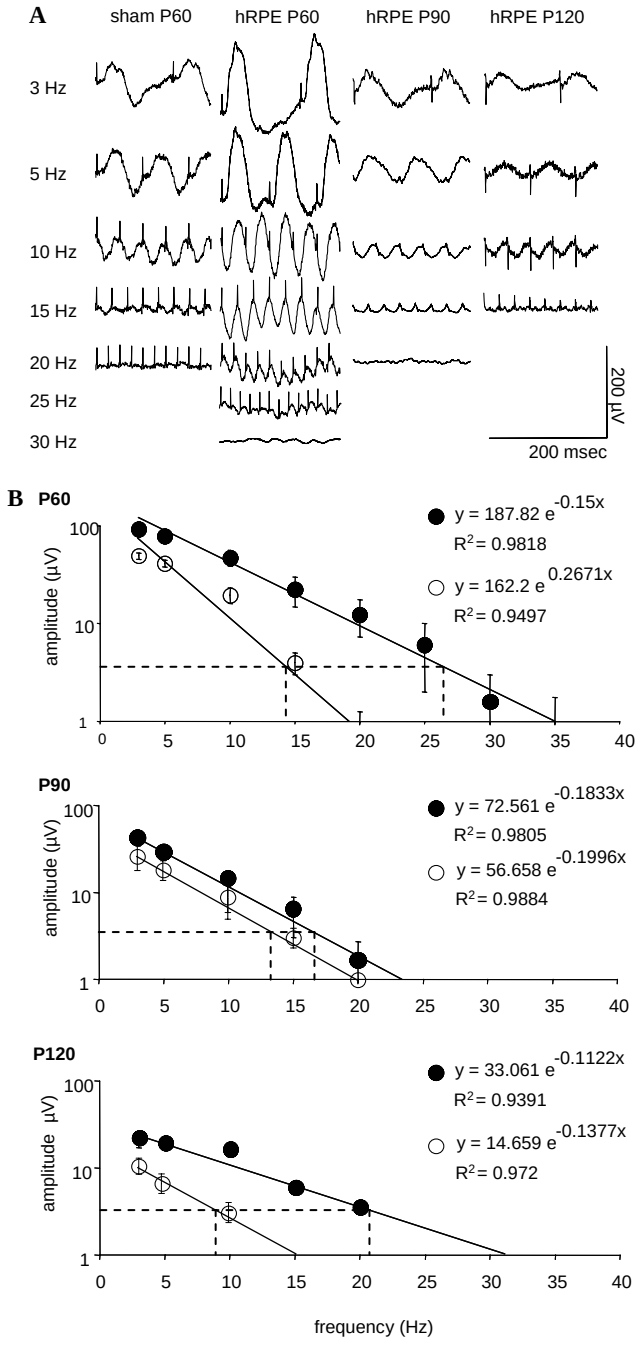

Fig. 5. (A) Examples of light-adapted flicker ERG responses recorded from the same animals and at the same time points as presented in Fig. 2. Higher amplitudes as well as higher CFF can be seen when comparing the hRPE-injected eye with the sham-injected eye at the P60 time point. There is a severe drop for both amplitude and CFF between P60 and P90 in the hRPE-injected eye. (B) Amplitude of the flicker ERG response as a function of stimulus frequency for animals recorded at ages P60, P90, and P120. Black circles: hRPE-injected eyes; white circles: sham eyes. Note that due to the use of log units on the ordinates, differences between individual data points are greater than they appear; this is especially true for higher values. Error bars represent the standard error of the mean.

b-wave amplitude elicited by the first flash, and therefore it was usually more prominent in treated eyes since they retained significantly higher b-wave amplitudes to a single flash. Under scotopic conditions, sham-injected animals showed the first indication of a b-wave (3 µV criterion amplitude) at 30 ms; the levels obtained to the second flash actually transiently exceeded by up to 5-fold the levels achieved with a single flash. In age-matched hRPE-injected animals, the first signs of a b-wave were only seen at 10 s and full recovery was not attained even after 120 s (not illustrated). By P90 in hRPE-injected eyes, the amplitude levels at various times following the conditioning flash under photopic adaptation were comparable to those seen in shams at P60, suggesting a deterioration with post-operative time. Such deterioration was less evident under scotopic adaptation. Interestingly, in all cases, the optimal b-wave response was systematically reached with a 120-ms delay following the conditioning flash. Due to a technical problem, photopic recovery experiments in hRPE-injected eyes could not be done at P120. Since no b-wave could be elicited to a single flash without a precedent conditioning flash at P90 and P120, recovery analysis was not undertaken at these time points in sham-injected eyes.

4. Discussion

Using the RCS rat as a model of progressive retinal degeneration caused by RPE dysfunction, the present study details what parameters of the ERG response are rescued after introduction of ARPE-19 cells to the subretinal space to rescue photoreceptors and how rescue characteristics change over the first 3 months post-transplantation. These observations form part of a series of studies examining the consequences of photoreceptor degeneration and rescue on downstream circuitry (Villegas-Perez, Lawrence, Vidal-Sanz, Lavail, & Lund, 1998; Wang, Lu, & Lund, 2005; Wang, Lu, Wood, & Lund, 2005) and on centrally mediated visual functions (Girman et al., 2003, 2005; McGill et al., 2004; Sauvé et al., 2002, 2004). The present ERG studies show that subretinal injections of the hRPE cell line ARPE-19 can maintain both rod- and cone-driven activity as evidenced by preserved ERG responsiveness. However, at the earliest time point tested (60 days of age), the amplitudes of the preserved ERG responses are at least 80% smaller than in non-dystrophics and drop even further by the second time point tested (90 days of age). Nevertheless, oscillatory potentials are recordable through the time period studied.

4.1. Relation to morphology

Fundamental to any changes seen in the ERG are those occurring in the retinal morphology, particularly the pattern of survival of rods and cones over the timescale examined here and the effects of transplantation on downstream events within the retina. These have been explored in parallel studies using the same animal strain and experimental conditions as in the present study. In the untreated dystrophic RCS rat, there are changes in the outer segment appearance as early as P16 and photoreceptor cell death is first seen shortly after the time of transplantation at P21. By P60, the outer nuclear layer is reduced from 10–14 cells

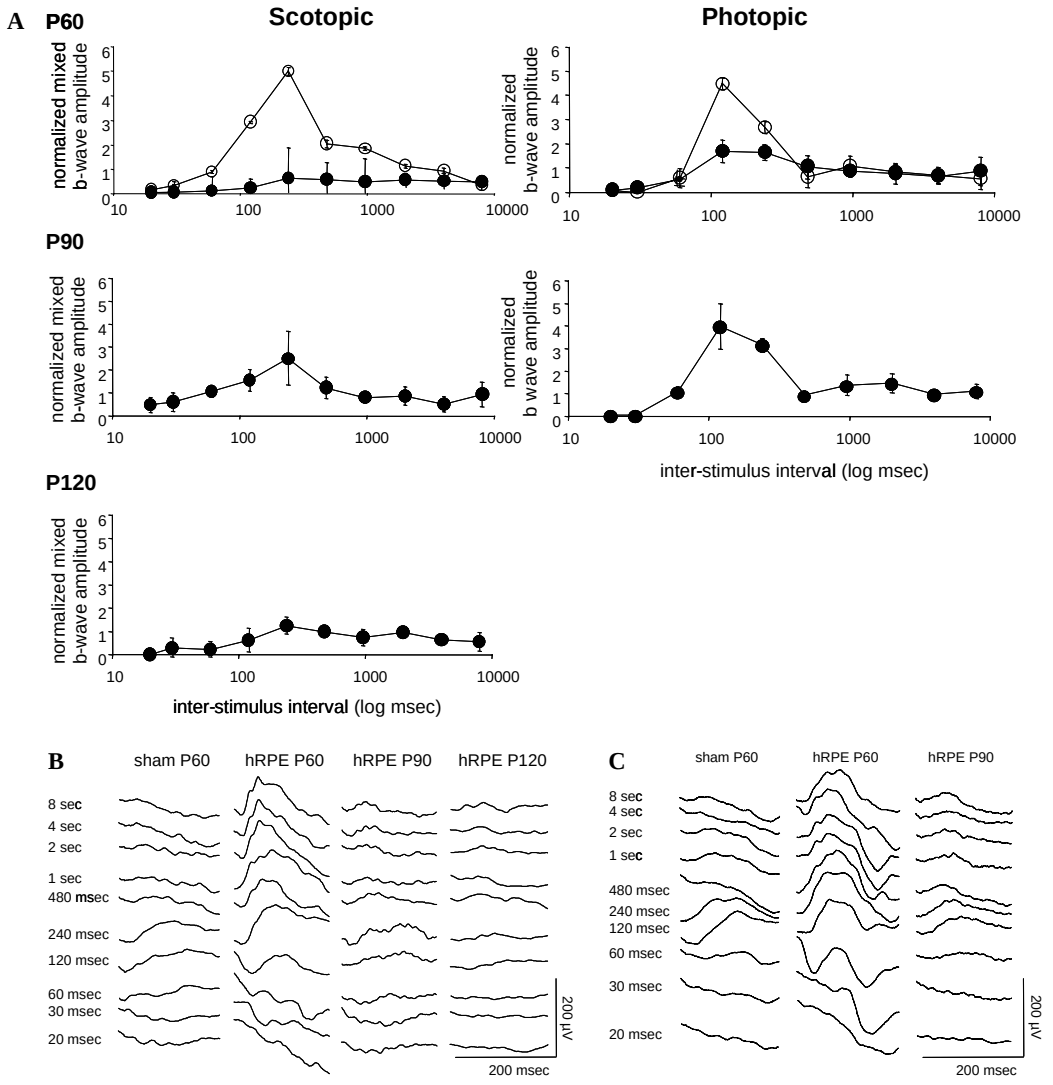

Fig. 6. (A) Time course of b-wave recovery from a conditioning flash. *y*-Axis represents the normalized amplitude of b-waves elicited by a probe flash (normalized the amplitude of responses to a probe flash not preceded by a conditioning flash) and the *x*-axis represents the delay (in log units) between both flashes. Graphs on the left are for mixed scotopic b-waves and right-hand graphs are for photopic b-waves. Black circles: hRPE-injected eyes; white circles: sham-injected eyes. Note the overshoot in normalized amplitudes (exceeding amplitudes of responses to a probe flash alone) exacerbated in sham-injected eyes at P60. Such overshoot is not seen in hRPE-injected eyes even at P120. Recovery experiments could not be done in sham-injected eyes at P90 and P120 since no b-waves could be elicited at these time points. (B) Under scotopic adaptation, examples of responses elicited by a probe flash (1.4 log cds/m^2) presented at increasing delays (from bottom to top) following the presentation of a conditioning flash (1.4 log cds/m^2). Traces are from the same animals and at the same time points as presented in Fig. 2. (C) Under photopic adaptation (30 cd/m^2), examples of responses elicited by a probe flash (1.4 log cds/m^2) presented at increasing delays (from bottom to top) following the presentation of a conditioning flash (1.4 log cds/m^2). Traces are from the same animals and at the same time points as presented in Fig. 2. Error bars represent the standard error of the mean.

thick down to 4–5 cells thick. By P90, it is further reduced to 1–2 cells thick and by P120, only scattered cells are seen: these are mainly cones (Cuenca, Pinilla, Sauvé, & Lund, 2005; Wang et al., 2005). Associated with this loss of photoreceptors, there is a progressive disarray of synaptic markers in the outer plexiform layer and by P60, a reduction in the complexity of bipolar cell dendrites. By P90, substantial sprouting of both bipolar cell dendrites occurs and horizontal cell processes into the debris zone formed by shed outer segments that could not be processed by RPE cells. This sprouting is not accompanied by an exuberance of synaptic marker expression. As the debris zone disappears by P120, the sprouting of these processes diminishes.

After transplantation at P21–23 of ARPE-19 cells into the upper temporal retina, rescue of photoreceptors is achieved with an outer nuclear layer up to eight cells thick at P60 reducing to a maximum of six cells deep at P120. Moving away from the area of best rescue, the thickness of the outer nuclear layer becomes progressively reduced so that in the lower nasal retina, distant from the site of graft introduction the retina appears very similar to an un-operated dystrophic animal. The area of rescue has been examined in several studies (Keegan, Sauvé, Winton, Coffey, & Lund, 2000; Keegan et al., 2005; Sauvé, Klassen, Whiteley, & Lund, 1998; Sauvé et al., 2004). At best, it occupies about 30% of the total retinal area. In several cases where serial

recording was made detailing the area of functional rescue over time, there was indication of a reduction from 30 to 10%. Recent work (Wang, Lu, Wood, et al., 2005) has shown reduction in the area of retina rescued over time and a concomitant loss of donor cells. Interestingly, rescue extended beyond the area of distribution of donor cells raising the possibility that the rescue effect may involve diffusible factors, and not simply cell contact-mediated processes. The changes seen in un-operated rats in bipolar dendrites and horizontal cell processes are largely prevented by cell transplantation (Wang, Lu, Wood, et al., 2005). Detailed study of synaptic markers in the outer plexiform layer (Lund et al., 2004; I. Pinilla, unpublished observations) has shown that while the numbers of matched pre- and post-synaptic profiles are reduced, they do maintain a normal order through at least P120.

4.2. Congenic non-dystrophic RCS rats

While normal rats have been extensively studied with ERG recordings, there are no published data on intensity responses obtained individually for rods and cones under scotopic adaptation conditions. Using a double-flash approach, we found that saturation of the cone responses is achieved at the beginning of the second rising phase in mixed scotopic intensity responses. The observation that the plateau of the second rising phase, in isolated rod responses, is reduced (in comparison with mixed scotopic intensity responses) by about the same amplitude as isolated cone responses suggests that cones are the major contributor to this second phase.

4.3. Sham treatment

As previously reported in untreated dystrophic RCS rats (Bush et al., 1995; Pinilla et al., 2004; Sauvé et al., 2004), mixed scotopic a- and b-waves, respectively, vanish by P60 and P90 in sham-injected eyes. Also as seen in untreated rats (Cuenca et al., 2005), no oscillatory potentials can be recorded by P60, either under scotopic or photopic adaptation. The only ERG responses recorded in sham-injected eyes at P90 or P120 are elicited by flicker stimuli: this is consistent with anatomical and functional evidence that cones are the last type of photoreceptor to persist in late degenerative stages in RCS rats (Cotter and Noell, 1984; Girman et al., 2005; LaVail et al., 1974; Pinilla et al., 2004, 2005).

A unique characteristic of the sham-injected eyes is the occurrence, both under scotopic and photopic adaptation, of a high threshold STR-like negative component at P60 up to P120. In hRPE-injected animals such negative waves are not seen until P120, and then only in a single animal of the six analyzed at that age. The STR represents activity from RGCs (Bui & Fortune, 2004) and persists in RCS rats both under scotopic (Bush et al., 1995) and photopic (Sugawara, Machida, Sieving, & Bush, 1999) conditions, at an age when no other components can be elicited. The negative STR-like wave effectively reduces the mixed b-wave amplitude: intravitreal injections of *N*-methyl-DL-aspartic acid (NMA), which blocks activity from third-order neurons, increase the b-wave in 10-week-old RCS rats, suggesting that a negative STR-like component (driven by third-order neurons) is superimposed on the positive b-wave (Machida et al., 2001). Similar unmasking effects are obtained here using the double-flash approach supporting previous findings that STR-like generators can be bleached or saturated (Frishman & Sieving, 1995). Our studies of recovery dynamics from a conditioning flash indicate that unmasking (seen as an "overshooting" from normalized responses) is maximal at 120-ms intervals. The fact that "overshooting" is exacerbated in sham-injected animals indicates that the STR-like negative wave constitutes a larger proportion of the mixed responses than in hRPE-injected animals.

4.4. Subretinal hRPE injections

Our results show that following subretinal hRPE cell injections, the mixed b-waves recorded at P60 have a single rising phase but are still largely driven by rod-dependent activity. Although the rod contribution to the b-wave diminishes with time, double-flash-derived rod b-waves can still be recorded at P90 and P120, indicating that hRPE injections do preserve some degree of rod-driven ERG activity. However, the fact that the response abolished by the first flash comprises a negative component (instead of a positive going b-wave) suggests that rod-driven activity is abnormal; in non-dystrophics, the response abolished by the first flash comprises a positive going b-wave, which has been shown to be rod-driven in previous studies (Birch et al., 1995; Lyubarsky et al., 1999; Nixon et al., 2001). The observation that mixed scotopic responses can be elicited below cone threshold levels ($-1.63\,\log cds/m^2$ in non-dystrophics) gives additional support for the preservation of rod activity in hRPE-injected rats. In untreated dystrophic RCS rats, not only are rod-driven b-waves no longer recorded by P90 but also mixed scotopic and photopic b-waves themselves can no longer be elicited (Pinilla et al., 2004).

Although hRPE injections lead to the preservation of maximal rod and cone-driven b-wave amplitudes in comparison with sham-injections, the amplitudes of the sustained b-waves never exceed 20% of the values recorded in non-dystrophics; other parameters including CFFs and recovery dynamics are also abnormal. The ultimate measure of success is a comparison with untreated dystrophics, at weeks of age, the time of the preventive intervention. Recent studies (Cuenca et al., 2005; Pinilla et al., 2004) indicate that at this age, although cone-driven responses are normal, rod-driven responses already show signs of dysfunction when compared with age-matched non-dystrophic RCS rats. Taking maximal scotopic b-waves, their respective values are down from $990 \pm 50\,\mu V$ in P21 non-dystrophics to $658 \pm 66\,\mu V$ in P21 dystrophics, raising the percentage of rescued amplitude by a factor of 1.5. The

amplitude of the maximal b-waves maintained at P60 in hRPE-injected eyes in proportion to that obtained at P21 (the time of cell injections) in untreated dystrophics is still only 30%, suggesting only partial preservation. Several factors might be responsible for reduced amplitudes and abnormal response properties. These are discussed below:

4.4.1. Area of preserved retina

One reason for the small amplitudes of the sustained b-waves might be because cell injections preserve only a small part of the retina. Perimetry-like recordings in RCS rats (Sauvé, Girman, Wang, Lawrence, & Lund, 2001) indicate that hRPE injections do not rescue low threshold responses completely: in best cases, thresholds of 0.7 log cds/m^2 over background are recorded compared with non-dystrophics where figures of 0.3–0.5 are found (Sauvé et al., 2002). Second, as indicated above, both anatomical and functional rescue comprise less than 30% of the total retinal area (Sauvé et al., 2004; Wang, Lu, Wood, et al., 2005) and the area of rescue reduces with age. Since the corneal full field ERG reflects summation of activity from the whole eye, it is a reasonable assumption that under optimal rescue conditions (60 days of age) the amplitude of the signal might still achieve only a fraction of the signal generated by the whole retina in non-dystrophic RCS rats. Support for this hypothesis comes from recent studies (Sauvé et al., 2004) showing that the magnitude of the b-wave is proportional to the area and degree of visual field preservation.

4.4.2. Number of photoreceptors rescued

There are examples, including rat models of light damage and P23H dystrophy, showing a relationship between the decrease in a- and b-wave amplitudes and the combined effect of photoreceptor loss and reduction in outer segment length (Machida et al., 2000; Sugawara, Sieving, & Bush, 2000). On the other hand, there are also instances in which anatomical rescue is not accompanied by functional rescue. The effect of HSV vector-delivered FGF2 in the light-damaged retina of RCS rats (Spencer, Agarwala, Gentry, & Brandt, 2001) and the effect of CNTF delivered by recombinant adeno-associated virus in the retina of mice with a P216L rds/peripherin mutation (Bok et al., 2002) are two examples.

We have recently shown that following hRPE injections in RCS rats, rods rescued anatomically are dysfunctional (Girman et al., 2005) and their anatomical rescue is not in concert with rod ERG responses (Pinilla, Lund, Lu, et al., 2005). Although dysfunctional, the preserved rods might still play an essential role in sustaining cones by releasing diffusible factors (Leveillard et al., 2004), and as such, a higher number of anatomically preserved rods could result in better preservation of cone function. This being said, the present study provides evidence (summarized in Section 4.4) that although rod-driven activity is abnormal in hRPE-injected eyes, it is still recordable with full field ERG up to P120.

4.4.3. Defective phototransduction

Phototransduction events are thought to be directly reflected in the leading edge of the a-wave. At the time of injection, P21, this leading edge appears normal in dystrophic RCS rats (Y. Sauvé, unpublished results), offering the possibility of being maintained as such by preventive intervention. Although the small amplitude and saturation at low light levels of the rescued a-waves precludes a thorough analysis of their leading edge, normalized a-wave leading edges (amplitudes normalized against respective maximal amplitudes) in hRPE-injected dystrophics at P60 show similar leading edges up to 10 ms as in age-matched non-dystrophics, but followed from 10 to 15 ms by an aberrant deflection (see Fig. 7 for an example of a sustained a-wave with maximal amplitude obtained at 0.38 log cds/m^2 compared with an a-wave obtained in a non-dystrophic rat with the same stimulus luminance). Since all hRPE-injected eyes retained an a-wave at P60, we were able to compare their normalized shape and found that at P60 seven out of the 12 hRPE-injected eyes had similar deflections as for the example shown in Fig. 7, albeit with slight variations in onset, slope, and duration. Therefore, it is possible that part of the initial phototransduction steps might be unaffected in rescued photoreceptors capable of phototransduction.

The inability of individual photoreceptors to phototransduce light signals appropriately will have repercussions on other ERG components such as the b-wave. The injected cells might not allow restoration of the normal relationship between RPE and photoreceptors which is required for photopigment recycling, a crucial step in phototransduction. In addition to having significantly reduced amplitudes, in comparison with non-dystrophics, the b-waves sustained following subretinal hRPE injections in dystrophic RCS rats saturate at lower flash intensities than in non-dystrophics (especially for rod b-waves) and plummet in amplitudes at higher intensities, suggesting that the rescued rods are more sensitive to light bleaching than in non-dystrophics. Recordings from untreated dystrophic

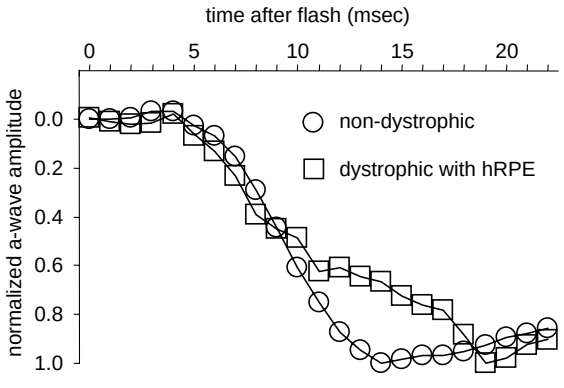

Fig. 7. Example of an a-wave sustained at P60 following hRPE injection in a dystrophic RCS rat (square symbols) compared with an a-wave from a non-dystrophic RCS rat. Amplitude values are normalized for respective maximal amplitudes; absolute amplitude values: 32 and 418 μV in the dystrophic and non-dystrophic animals, respectively. Stimulus luminance: 0.38 log cds/m^2.

RCS rats (Cuenca et al., 2005) indicate that such dysfunctional feature is not seen at P21 (the time cell injection was done in this study) but is already obvious at P30. This rapid deterioration in rod-responsiveness might not be avertable with a therapeutic intervention. Moreover, several studies imply that rods have various dysfunctional aspects at P21 in dystrophic RCS rats (Girman et al., 2005; Ohguro, Ohguro, Mamiya, Maeda, & Nakazawa, 2003) and consequently achievement of rod function to the levels seen in non-dystrophic rats is unfeasible using preventive intervention at P21. Nonetheless, rods can be preserved anatomically up to 7 months of age (Girman et al., 2005), but they are usually devoid of any segments and rhodopsin accumulates in their soma (Wang et al., 2005).

4.4.4. Modification at the synaptic level between photoreceptors and bipolar cells

Pharmacological manipulations have pointed to the essential role of ON bipolar cell activity in generating and contributing in a significant way to ERG b-waves (Stockton & Slaughter, 1989). Lower synaptic pairing between photoreceptors and bipolar cells might compromise ON bipolar activation as in non-dystrophics, and therefore lead to lower amplitude b-waves. Anatomical investigation of the animals used in this study (Lund et al., 2004) show that many of the retinal changes seen consequent to photoreceptor loss are largely prevented in the area of photoreceptor rescue even though the photoreceptor layer was reduced in thickness. One notable change, however, was the frequency of paired photoreceptor/bipolar synaptic markers in the outer plexiform layer. The anatomical observations of this and a parallel study (Lund et al., 2004) do not predict the large reduction in ERG response amplitudes nor the substantial deterioration between P60 and P90.

4.4.5. Inner retinal changes

The area of optimal photoreceptor rescue is also accompanied by preservation of the bipolar cell branching pattern, but not to the extent seen in non-dystrophics (Wang et al., 2005). The inability of the hRPE-injections to completely prevent changes in bipolar cells and other inner nuclear layer cells might also contribute to their inability to maintain the b-wave amplitudes to the levels seen in non-dystrophics.

4.5. Discrepancy between ERG and functional preservation at the CNS level

Light- and dark-adaptation studies, using multi-unit recordings defined visual receptive fields in the superior colliculus of RCS rats following hRPE injections, indicate that these animals are essentially "night blind" despite the persistence of rods up to 7 months of age (Girman et al., 2005). Therefore, although rod-driven activity can be recorded even at low luminance level, as indicated by full field ERG results, such information might not be processed appropriately under physiological conditions to drive central visual functions. Isolated cone b-waves do not show signs of bleaching, either under scotopic or photopic adaptation. Intensity-response curves for isolated dark-adapted cone b-waves are similar to those for photopic b-waves, suggesting that the double-flash protocol used here is reliable in extracting the cone-driven contribution from the mixed scotopic ERG. Although both maximal amplitudes and CFFs are significantly higher in hRPE-injected compared with age-matched sham-injected eyes, there is an obvious deterioration in cone responses with age, especially from P60 to P90. Studies by Xu et al. (2003) and Pinto et al. (2004) might suggest that the background light used here ($30\,cds/m^2$) to record cone responses on a rod suppressing background may be too bright. However, this is unlikely since the double-flash-isolated cone responses under dark-adaptation gave similar results as under photopic adaptation. Furthermore, this decline in cone function is consistent with findings from perimetry-like recordings in the superior colliculus (under mesopic adaptation) pointing to a significant elevation in visual thresholds from P60 to P90, both in terms of levels and area (Keegan et al., 2000, 2005). However, there are no indications of such decline in cortically dependent visual function, such as with recordings of visual responses from the primary visual cortex (Girman et al., 2003) or behavioral measures of acuity (McGill et al., 2004). Whether this discrepancy between retina-related functional tests (ERG and perimetry-like threshold responses) and cortically related functional tests reflects changes in gain between retina and cortex is unclear. Part of the explanation might be related to the fact that full field ERG responsiveness reflects averaged response from the whole retina while behavioral measures of acuity might depend on the a defined area of the retina with optimal functional preservation. For instance, patients with advanced RP might have a flat ERG but still retain good vision over a small area of their central visual field.

5. Conclusion

Our findings indicate that both rod- and cone-related ERG responsiveness can be preserved by subretinal hRPE cell injections. However, the magnitude of the ERG responses represents only a fraction of that seen in non-dystrophics. Furthermore, there is a severe decline in both rod- and cone-driven ERG responsiveness from P60 to P90. The relation between ERG results and those obtained with other indices (both morphological and functional) suggest a dynamic interplay among these various parameters in the rescue process.

Acknowledgments

The authors thank Dr. S. Wang for preparing the human RPE cells and Dr. B. Lu for injecting them in the subretinal space of RCS rats. This work was supported by NIH (EY14038), FFB (Foundation to Fight Blindness), Wynn Foundation, and RPB grants. I. Pinilla was supported by

grants from the Spanish Government (FIS 02/5010 and BA03/0016).

References

Birch, D. G., Hood, D. C., Nusinowitz, S., & Pepperberg, D. R. (1995). Abnormal activation and inactivation of rod transduction in patients with autosomal dominant retinitis pigmentosa and the Pro-23-His mutation. *Investigative Ophthalmology and Visual Science, 36*, 1603–1614.

Bok, D., Yasumura, D., Matthes, M. T., Ruiz, A., Duncan, J. L., Chappelow, A. V., et al. (2002). Effects of adeno-associated virus-vectored ciliary neurotrophic factor on retinal structure and function in mice with a P216L rds/peripherin mutation. *Experimental Eye Research, 74*, 719–735.

Bourne, M. C., Campbell, D. A., & Tansley, K. (1938). Hereditary degeneration of the rat retina. *British Journal of Ophthalmology, 22*, 613–623.

Bui, B. V., & Fortune, B. (2004). Ganglion cell contributions to the rat full-field electroretinogram. *Journal of Physiology, 555*, 153–173.

Bush, R. A., Hawks, K. W., & Sieving, P. A. (1995). Preservation of inner retinal responses in the aged Royal College of Surgeons rat. Evidence against glutamate excitotoxicity in photoreceptor degeneration. *Investigative Ophthalmology and Visual Science, 36*, 2054–2062.

Coffey, P. J., Girman, S., Wang, S. M., Hetherington, L., Keegan, D. J., Adamson, P., et al. (2002). Long-term preservation of cortically dependent visual function in RCS rats by transplantation. *Nature Neuroscience, 5*, 53–56.

Cotter, J. R., & Noell, W. K. (1984). Ultrastructure of remnant photoreceptors in advanced hereditary retinal degeneration. *Investigative Ophthalmology and Visual Science, 25*, 1366–1375.

Cuenca, N., Pinilla, I., Sauvé, Y., & Lund, R. D. (2005). Changes in synaptic connectivity following progressive photoreceptor degeneration in RCS rats. *European Journal of Neuroscience, 22*, 1057–1072.

D'Cruz, P. M., Yasumura, D., Weir, J., Matthes, M. T., Abderrahim, H., LaVail, M. M., et al. (2000). Mutation of the receptor tyrosine kinase gene Mertk in the retinal dystrophic RCS rat. *Human Molecular Genetics, 9*, 645–651.

Dowling, J. E., & Sidman, R. L. (1962). Inherited retinal dystrophy in the rat. *Journal of Cell Biology, 14*, 73–109.

Fishman, G. A., Birch, D. G., Holder, G. E., & Brigell, M. G. (2001). *Electrophysiologic testing in disorders of the retina, optic nerve, and visual pathway* (2nd ed.). San Francisco, CA: American Academy of Ophthalmology.

Frishman, L. J., & Sieving, P. A. (1995). Evidence for two sites of adaptation affecting the dark-adapted ERG of cats and primates. *Vision Research, 35*, 435–442.

Gal, A., Li, Y., Thompson, D. A., Weir, J., Orth, U., Jacobson, S. G., et al. (2000). Mutations in MERTK, the human orthologue of the RCS rat retinal dystrophy gene, cause retinitis pigmentosa. *Nature Genetics, 26*, 270–271.

Girman, S. V., Wang, S., & Lund, R. D. (2003). Cortical visual functions can be preserved by subretinal RPE cell grafting in RCS rats. *Vision Research, 43*, 1817–1827.

Girman, S. V., Wang, S., & Lund, R. D. (2005). Time course of deterioration of rod and cone function in RCS rat and the effects of subretinal cell grafting: A light- and dark-adaptation study. *Vision Research, 45*, 343–354.

Gouras, P., & MacKay, C. J. (1989). Growth in amplitude of the human cone electroretinogram with light adaptation. *Investigative Ophthalmology and Visual Science, 30*, 625–630.

Gu, S. M., Thompson, D. A., Srikumari, C. R., Lorenz, B., Finckh, U., Nicoletti, A., et al. (1997). Mutations in RPE65 cause autosomal recessive childhood-onset severe retinal dystrophy. *Nature Genetics, 17*, 194–197.

Keegan, D. J., Sauvé, Y., Winton, H., Coffey, P. J., & Lund, R. D. (2000). Visual field preservation and anatomical rescue after transplantation of immortalized RPE cells in the RCS rat. *Investigative Ophthalmology and Visual Science, 41*, S857.

Keegan, D. J., Gias, C., Sauvé, Y., Lund, R., Greenwood, J., & Coffey, P. (2005). Correlation of Preserved Retinal Structure and Function in the RCS Rat. *Investigative Ophthalmology and Visual Science, 46*, S4140.

LaVail, M. M., Sidman, M., Rausin, R., & Sidman, R. L. (1974). Discrimination of light intensity by rats with inherited retinal degeneration: A behavioral and cytological study. *Vision Research, 14*, 693–702.

Leveillard, T., Mohand-Said, S., Lorentz, O., Hicks, D., Fintz, A. C., Clerin, E., et al. (2004). Identification and characterization of rod-derived cone viability factor. *Nature Genetics, 36*, 755–759.

Lund, R. D., Adamson, P., Sauvé, Y., Keegan, D. J., Girman, S. V., Wang, S., et al. (2001). Subretinal transplantation of genetically modified human cell lines attenuates loss of visual function in dystrophic rats. *Proceedings of the National Academy of Sciences of the United States of America, 98*, 9942–9947.

Lund, R. D., Pinilla, M. I., Sauvé, Y., Wang, S., Lu, B., & Cuenca, N. (2004). Effect of human RPE cell line transplantation on synaptic relay in RCS rats. *Investigative Ophthalmology and Visual Science, E Abstract, 5176*.

Lyubarsky, A. L., Falsini, B., Pennesi, M. E., Valentini, P., & Pugh, E. N., Jr. (1999). UV- and midwave-sensitive cone-driven retinal responses of the mouse: A possible phenotype for coexpression of cone photopigments. *Journal of Neurosciences, 19*, 442–455.

Machida, S., Kondo, M., Jamison, J. A., Khan, N. W., Kononen, L. T., Sugawara, T., et al. (2000). P23H rhodopsin transgenic rat: Correlation of retinal function with histopathology. *Investigative Ophthalmology and Visual Science, 41*, 3200–3209.

Machida, S., Chaudhry, P., Shinohara, T., Singh, D. P., Reddy, V. N., Chylack, L. T., Jr., et al. (2001). Lens epithelium-derived growth factor promotes photoreceptor survival in light-damaged and RCS rats. *Investigative Ophthalmology and Visual Science, 42*, 1087–1095.

Marlhens, F., Bareil, C., Griffoin, J. M., Zrenner, E., Amalric, P., Eliaou, C., et al. (1997). Mutation in RPE65 cause Leber's congenital amaurosis. *Nature Genetics, 17*, 139–141.

Maw, M. A., Kennedy, B., Knight, A., Bridges, R., Roth, K. E., Mani, E. J., et al. (1997). Mutation of the gene encoding cellular retinal-aldehyde-binding protein in autosomal recessive retinitis pigmentosa. *Nature Genetics, 17*, 198–200.

McGill, T. J., Lund, R. D., Douglas, R. M., Wang, S., Lu, B., & Prusky, G. T. (2004). Preservation of vision following cell-based therapies in a model of retinal degenerative disease. *Vision Research, 44*, 2559–2566.

McHenry, C. L., Liu, Y., Feng, W., Nair, A. R., Feathers, K. L., Ding, X., et al. (2004). MERTK arginine-844-cysteine in a patient with severe rod-cone dystrophy: Loss of mutant protein function in transfected cells. *Investigative Ophthalmology and Visual Science, 45*, 1456–1463.

Nandrot, E., Dufour, E. M., Provost, A. C., Pequignot, M. O., Bonnel, S., Gogat, K., et al. (2000). Homozygous deletion in the coding sequence of the c-mer gene in RCS rats unravels general mechanisms of physiological cell adhesion and apoptosis. *Neurobiology of Diseases, 7*, 586–599.

Nixon, P. J., Bui, B. V., Armitage, J. A., & Vingrys, A. J. (2001). The contribution of cone responses to rat electroretinograms. *Clinical and Experimental Ophthalmology, 29*, 193–196.

Nusinowitz, S., Ridder, W. H., & Heckenlively, J. R. (2002). Electrophysiological testing of the mouse visual system. In R. S. Smith (Ed.), *Systematic evaluation of the mouse eye: Anatomy, pathology, and biomethods* (pp. 320–344). Boca Raton, FL: CRC Press.

Ohguro, H., Ohguro, I., Mamiya, K., Maeda, T., & Nakazawa, M. (2003). Prolonged survival of the phosphorylated form of rhodopsin during dark adaptation of Royal College Surgeons rat. *FEBS Letters, 551*, 128–132.

Peachey, N. S., Goto, Y., al-Ubaidi, M. R., & Naash, M. I. (1993). Properties of the mouse cone-mediated electroretinogram during light adaptation. *Neuroscience Letter, 162*, 9–11.

Peachey, N. S., & Ball, S. L. (2003). Electrophysiological analysis of visual function in mutant mice. *Documenta Ophthalmologica, 107*, 13–36.

Perlman, I. (1978). Kinetics of bleaching and regeneration of rhodopsin in abnormal (RCS) and normal albino rats in vivo. *Journal of Physiology, 278*, 141–159.

Petrukhin, K., Koisti, M. J., Bakall, B., Li, W., Xie, G., Marknell, T., et al. (1998). Identification of the gene responsible for Best macular dystrophy. *Nature Genetics, 19*, 241–247.

Pinilla, I., Lund, R. D., & Sauvé, Y. (2004). Contribution of rod and cone pathways to dark-adapted electroretinogram (ERG) b-wave following retinal degeneration in RCS rats. *Vision Research, 44*, 2467–2474.

Pinilla, I., Lund, R. D., Lu, B., & Sauvé, Y. (2005). Measuring the cone contribution to the ERG b-wave to assess function and predict anatomical rescue in RCS rats. *Vision Research, 45*, 635–641.

Pinilla, I., Lund, R. D., & Sauvé, Y. (2005). Cone function studied with flicker electroretinogram during progressive retinal degeneration in RCS rats. *Experimental Eye Research, 80*, 51–59.

Pinto, L. H., Vitaterna, M. H., Siepka, S. M., Shimomura, K., Lumayag, S., Baker, M., et al. (2004). Results from screening over 9000 mutation-bearing mice for defects in the electroretinogram and appearance of the fundus. *Vision Research, 44*, 3335–3345.

Raibon, E., Roger, M., & Lund, R. D. (2003). Effects of dexamethasone on microglial activation in rats with inherited retinal dystrophy. *Society for Neuroscience Abstract, 103.3*.

Sauvé, Y., Klassen, H., Whiteley, S. J. O., & Lund, R. D. (1998). Visual field loss in RCS rats and the effect of RPE cell transplantation. *Experimental Neurology, 152*, 243–250.

Sauvé, Y., Girman, S. V., Wang, S., Lawrence, J. M., & Lund, R. D. (2001). Progressive visual sensitivity loss in the Royal College of Surgeons rat: Perimetric study in the superior colliculus. *Neuroscience, 103*, 51–63.

Sauvé, Y., Girman, S. V., Wang, S., Keegan, D. J., & Lund, R. D. (2002). Preservation of visual responsiveness in the superior colliculus of RCS rats after retinal pigment epithelium cell transplantation. *Neuroscience, 114*, 389–401.

Sauvé, Y., Lu, B., & Lund, R. D. (2004). The relationship between full field electroretinogram and perimetry-like visual thresholds in RCS rats during photoreceptor degeneration and rescue by cell transplants. *Vision Research, 44*, 9–18.

Spencer, B., Agarwala, S., Gentry, L., & Brandt, C. R. (2001). HSV-1 vector-delivered FGF2 to the retina is neuroprotective but does not preserve functional responses. *Molecular Therapy, 3*, 746–756.

Stockton, R. A., & Slaughter, M. M. (1989). B-wave of the electroretinogram. A reflection of ON bipolar cell activity. *Journal of General Physiology, 93*, 101–122.

Sugawara, T., Machida, S., Sieving, P. A., & Bush, R. A. (1999). The photopic ERG of the light-damaged and RCS rat: Persistence of a negative component from the inner retina. *Investigative Ophthalmology and Visual Science, 40*, S22.

Sugawara, T., Sieving, P. A., & Bush, R. A. (2000). Quantitative relationship of the scotopic and photopic ERG to photoreceptor cell loss in light damaged rats. *Experimental Eye Research, 70*, 693–705.

Thompson, D. A., McHenry, C. L., Li, Y., Richards, J. E., Othman, M. I., Schwinger, E., et al. (2002). Retinal dystrophy due to paternal isodisomy for chromosome 1 or chromosome 2, with homoallelism for mutations in RPE65 or MERTK, respectively. *American Journal of Human Genetics, 70*, 224–229.

Villegas-Perez, M. P., Lawrence, J. M., Vidal-Sanz, M., Lavail, M. M., & Lund, R. D. (1998). Ganglion cell loss in RCS rat retina: A result of compression of axons by contracting intraretinal vessels linked to the pigment epithelium. *Journal of Comparative Neurology, 392*, 58–77.

Wang, S., Lu, B., & Lund, R. D. (2005). Morphological changes in the RCS retina during photoreceptor degeneration and after cell-based therapy. *Journal of Comparative Neurology, 491*, 400–417.

Wang, S., Lu, B., Wood, P., & Lund, R. D. (2005). Grafting of ARPE-19 and Schwann cells to the subretinal space in RCS rats. *Investigative Ophthalmology and Visual Science, 46*, 2552–2560.

Xu, L., Ball, S. L., Alexander, K. R., & Peachey, N. S. (2003). Pharmacological analysis of the rat cone electroretinogram. *Visual Neuroscience, 20*, 297–306.